Egypt. J. Chem. **Vol. 63,** No. 4, pp.1149-1159 (2020)

Egyptian Journal of Chemistry
http://ejchem.journals.ekb.eg/

Vibrational Spectra, Normal Coordinate Analysis, and Structure of Keto Form of Acetylacetone: A DFT Approach

Sepideh Mehrani[1, *], Sayyed Faramarz Tayyari[1], Mohammad Momen Heravi[1], Ali Morsali[1]

[1] *Chemistry Department, Mashhad Branch, Islamic Azad University, Mashhad, Iran*

IN this paper, we discuss the stability, structure, and vibrational assignment of possible keto forms (Ket1 and Ket2) of acetylacetone, AA, in the gas phase and solutions. The geometry optimization and harmonic and anharmonic vibrational frequencies are calculated at the B3LYP/6-311++G** level. In addition, we also optimize the molecular structure at the MP2/6-311++G(p,d) level. The investigation in solutions is carried out by means of the PCM-SCRF method. We study the relative stability of Ket1 and Ket2 in different media using B2PLYP/6-31+G(d,p) and CBS-QB3 levels. By comparing the IR spectra of AA in a polar solvent, CH_3CN, and a nonpolar solvent, CCl_4, and considering the theoretical results, the vibrational band frequencies of both keto and enol tautomers are distinguished. Our calculations and vibrational spectra confirm the coexisting of two keto forms in the solutions, designated as Ket1 and Ket2. According to both theoretical and experimental results, Ket1 and Ket2 are predominant in the nonpolar and polar solutions, respectively. In addition, we also do a normal coordinate analysis by using the normal mode eigenvectors obtained at the B3LYP/6-311++ G(d,p) level. The observed vibrational wavenumbers, IR and Raman relative intensities, and Raman depolarization ratios of AA and its deuterated analogous agree satisfactorily with the calculated results obtained at the B3LYP/6-311++G(d,p) method.

Keywords: Acetylacetone, Keto form, Normal coordinate analysis (NCA), Vibrational assignments, Tautomerization, Density Functional Theory

Introduction

β-Diketones are a class of compounds that the two carbonyl groups are separated by a $-CX_2-$ group. If one of the X atoms is hydrogen, then the compound undergoes a keto-enol tautomerization. The position of tautomerization is determined by several parameters, such as temperature [1-3], state of samples [4-7], nature of solvent [8-12], concentration [13], and substitution on the α- and β-positions [14-19]. The vibrational spectra of the enol form of several β-diketones have been extensively investigated several decades [20-34]. In an extensive work, Tayyari and Milani-Nejad [21] considered the vibrational spectra and possible stable structures of the enol form of acetylacetone. In this study, three enol forms of acetylacetone, which aroused from the rotation of CH_3 groups, were reported, which their energies are very close with each other. However, these conformers are the transition states of the most stable enol forms and they are not stable species. However, according to our knowledge, there is no theoretical or experimental work on the vibrational spectra of the keto forms of β-diketones, except a report on the IR and Raman wavenumber of AA in the keto form by Ernstbrunner [29]. Since in water solution the keto form is predominant, Ernstbrunner

Corresponding author: Sepideh Mehrani, e-mail: Sepideh_mehrani@yahoo.com, Phone +98 1732254163
Received 26/06/2019; Accepted 06/09/2019
DOI: 10.21608/ejchem.2019.13578.1868

[29], by comparing the IR and Raman spectra of AA in the CCl_4 and H_2O solutions, could distinguish the vibrational band frequencies of keto form from those of the enol form. However, Ernstbrunner [29] tentatively assigned some of the observed vibrational wavenumbers of the keto form.

Several authors [35-37] considered only one keto form in the gas phase and in solutions. On the other hand, Schlund et al. [38], by considering one enol and two keto forms, studied the keto-enol tautomerization of the titled compound by using DFT (RI-BP86, B3LYP, BHLYP levels) and ab initio HF and MP2 method by single point calculations using several basis sets. These authors used the CPCM method to calculate the energies in solutions. Schlund et al. [38] concluded that the B3LYP level overestimates the enol content and MP2 overestimates the keto content in the samples. McCann et al. [39] also used numerous modern methods to calculate the enol and keto contents of several molecules, including AA, and showed that CBS gives reasonable results for calculating the keto-enol content. However, these authors also considered only one conformer for the keto form of AA.

The aim of this work is the normal coordinate analysis and assignments of the vibrational band frequencies of the keto forms (wavenumbers, IR band intensity, and Raman activities) of AA by the aid of density functional theory (DFT) approach.

Method of calculations

We perform all theoretical calculations using the Gaussian 09 program [40]. All the calculations (viz., conformational analysis, geometrical parameters, vibrational wavenumber, infrared and Raman intensities of the title compound) are carried out using the B3LYP [41,42, 43] level and 6-311++G(d,p) basis set. Since the solvent has a great effect on the position of keto-enol equilibrium, all calculations are performed in the gas phase as well as in CCl_4, CH_3CN, and H_2O solutions. The bulk solvent effect is described by the polarizable continuum method (PCM) [44,45] at 298.15 K and 1.0 atm by performing SCRF calculations at the B3LYP/6-311++G(d,p) level. It has been shown that the thermodynamics results obtained with the CBS-QB3 [46] and B2PLYP [47] levels are comparable with the experimental data [48-50]. Therefore, the relative stability of considered tautomers and the equilibrium constants between these tautomers in the gas phase as well as in the solutions are calculated at the CBS-QB3 and B2PLYP/6-31+G(2d,p) levels.

To confirm our assignments, the anharmonic [51] vibrational wavenumbers for the keto forms of AA and its partially deuterated analogous, d_2AA, in the H_2O solution are also calculated at the B3LYP/6-311++G(d,p) level.

The positive value of all calculated vibrational wavenumbers of both conformers confirms the stability of their optimized geometries. An empirical uniform scaling factor of 0.9859 up to 1700 cm^{-1} and 0.9609 for greater than 1700 cm^{-1} [52] was used for calculated harmonic vibrational frequencies to outweigh the systematic errors caused by the basis set incompleteness, neglect of electron correlation, Fermi resonance, and vibrational anharmonicity.

A normal coordinate analysis is carried out to provide a complete description of the fundamental vibrational wavenumbers for the Ket1 and Ket2 species and its deuterated analogous. The normal coordinates and potential energy distributions (PED) are calculated from appropriate combinations of internal coordinates obtained from the Gaussian outputs, as explained elsewhere [53–57]. The full sets of 50 standard internal coordinates containing 11 redundancies are defined as given in Table S1 (Supplementary material). From these internal coordinates, a non-redundant set of local symmetry coordinates is constructed by a suitable linear combination of internal coordinates, which is given in Table S1 (Supplementary material). By combining the results of GaussView program [58] with the PEDs, the vibrational descriptions are made with a high degree of accuracy. Vibrational assignments are based on the comparison of calculated and observed Raman [29] and IR frequencies and intensities. To determine the position of overlapped and hidden band frequencies in the C=O vibration region, Lorentzian function has been utilized for deconvolution of IR spectrum using the Microsoft® Office Excel spreadsheet software.

Experimental

AA, carbon tetrachloride and acetonitrile are obtained from Aldrich chemical company. The IR spectra are recorded on a Bomem B-154 Fourier Transform Spectrophotometer in the 4000–600 cm−1 region. The spectra are collected at 2 cm−1 resolution by co-adding the results of 15 scans.

The Far-IR spectra in the 600-300 cm-1 region are obtained using a Thermo Nicolet NEXUS 870 FT-IR spectrometer. The spectra are collected with a resolution of 2 cm-1 by averaging the results of 64 scans.

Results and Discussion

Geometry

By rotating the C=O and CH_3 groups around single bonds and fully optimization in the gas phase and in polar solutions, two keto conformers are found, which is in agreement with the Schlund et al. [38] results. These two keto conformers are designated as Ket1 and Ket2 which are shown in Fig. 1. The calculated geometrical parameters for these keto forms in the gas phase and H_2O solution are listed in Table 1. The standard Gibbs free energy difference and equilibrium constant for conversion of Ket1 to Ket2, calculated at the CBS-QB3 and B2PLYP/6-31+G(d,p) levels, are given in Table 2. As it is shown in this table, the Ket2 conformer is the predominant constituent in the polar solutions and is absent in the gaseous sample.

According to our calculations, the Ket2 dipole moment is about three times higher than that of Ket1(see Table 1). This is the reason for increasing the stability of Ket2 in the polar solution compared with Ket1.

Ket1 belongs to the C2 symmetry while Ket2 is C1. As it is shown in Table 1, the main differences between these two conformers are C1C2C3C4 and O1C2C4O2 dihedral angles. In Ket2 the oxygen atoms are closer to each other than those in Ket1. The O1C2C4O2 dihedral angle in Ket1 is about 140° and is almost independent of solvent polarity, while the value of this dihedral angle in Ket2 is highly solvent dependent and varies from 92.5° to 68.2° (MP2 calculations) by going from gas phase to the water solution (see Table 1). Another parameter which is affected by the media is the C=O bond length, which increases by increasing the solvent polarity, while almost all other bond lengths slightly decrease.

Vibrational assignment

Since in polar solutions Ket2 is the predominant keto form of AA, the vibrational band frequencies of keto form are discussed according to the calculated vibrational frequencies of Ket2. The calculated and observed vibrational wavenumbers along with their assignments for Ket2 are listed in Table 3. The corresponding assignments for Ket1 and its partially deuterated AA, d_2AA, and their normal modes are given in Tables S2 and S3 (supplementary materials). According to our observations and calculations, the vibrational band frequencies of enol and keto forms in the CH_3 stretching region are not distinguishable. Therefore, the CH_3 stretching region will not be considered. The simulated IR spectra of Ket1 and Ket2 are compared in Fig. 2. In Table 3, our assignments are compared with those tentatively suggested by Ernstbrunner [29].

C=O stretching region

The deconvoluted IR spectra of AA in the CH_3CN and CCl_4 solutions, in the 1750-1675 and 1350-1200 cm^{-1} regions, are compared in Fig. 3. As it is shown in Figs. 3a and 3b, there are three strong bands at 1728, 1709, and 1704 in CH_3CN solution and at 1731, 1712, and 1704 cm^{-1} in the CCl_4 solution. The second and third bands are assigned to the asymmetric C=O stretching of Ket2 and Ket1 species, respectively. The first band is caused by the superposition of the symmetric C=O stretching of both keto conformers. According to the theoretical calculations, the intensity of symmetric C=O stretching in Ket1 is one-tenth of that for Ket2 (see Fig. 2). By comparing the IR spectra of Ket1 and Ket2 in Fig. 3, it is concluded that the Ket1 content in the CH_3CN solution is considerably reduced compared to that in the CCl_4 solution. Therefore, the assignments for the keto form of AA in the CH_3CN and H_2O solutions in Table 3 are based on the vibrational frequencies of Ket2 conformer and the corresponding assignments for Ket1 are given in Table S2 (supplementary materials).

As it is shown in Fig. 2 and indicated in Table 3, a strong band at approximately 1300 cm^{-1} is predicted for the ket2 species which is absent in Ket1 conformer. This vibrational band is assigned to CH_2 wagging which is coupled to the C-C stretching and C=O bending modes. According to Figs. 3c and 3d, which compares the IR spectra of AA in CCl_4 and CH_3CN solutions in the 1340-1200 cm^{-1} region, the strong band at 1300 cm^{-1} is assigned to this mode of vibration in Ket2. The corresponding mode in Ket1 is expected to be observed at approximately 1240 cm^{-1} which is overlapped with one of the strong bands of the enol form.

Ogoshi and Nakamoto [34] considered the 1170 cm^{-1} band in the IR spectrum of gaseous acetylacetone as the superposition of two enol bands, CHα in-plane bending and one of the CH_3 rocking modes, while Ernstbrunner [29] assigned the 1170 cm^{-1} band to one of the enol bands, δCHα, and a band at 1159 cm^{-1} to the asymmetric CH_3 rocking mode in the keto tautomer. However, as it is shown in Fig. 4, deconvolution of the IR spectrum in the CCl_4 and CH_3CN solutions reveals three bands at 1185, 1170, and 1154 cm^{-1} in this region. The relative intensities of these bands vary from CCl_4 solution to CH_3CN solution. By considering the behavior of these bands with the change of solvent and our calculated results, the 1185 cm^{-1} band is assigned

TABLE 1. Selected geometrical parameters of Ket1 and Ket2 in the gas phase and water solution. [a]

	Ket1			Ket2			
	H_2O	Gas	H_2O	Gas	H_2O	Gas	H_2O
	A	A	B	B	A	B	B
R (Å)							
C1-C2	1.5052	1.5095	1.5055	1.5090	1.5073	1.5088	1.5066
C2-C3	1.5330	1.5359	1.5270	1.5296	1.5291	1.5233	1.5265
C3-C4	1.5330	1.5359	1.5270	1.5296	1.5210	1.5301	1.5157
C4-C5	1.5052	1.5095	1.5055	1.5090	1.5062	1.5121	1.5068
C2-O1	1.2156	1.2106	1.2225	1.2196	1.2159	1.2192	1.2225
C4-O2	1.2156	1.2106	1.2225	1.2196	1.2170	1.2186	1.2229
ϕ (°)							
C1C2C3	116.51	116.27	116.04	115.81	115.95	116.71	115.93
C2C3C4	109.48	108.42	107.06	106.11	112.78	111.71	110.76
C3C4C5	116.51	116.27	116.04	115.81	116.96	115.42	116.30
C1C2O1	122.87	123.10	123.29	123.47	122.48	123.12	121.19
C5C4O2	122.87	123.10	123.29	123.47	122.41	122.61	120.91
Δ (°)						MP2	
C1C2C3C4	88.68	89.19	88.32	88.21	172.81	162.06	169.11
C2C3C4C5	88.68	89.19	88.32	88.21	81.00	80.69	80.91
O1C2C1C4	179.30	178.40	178.45	177.56	179.81	179.56	179.94
O2C4C3C5	179.30	178.40	178.45	177.56	179.69	179.37	179.57
O1C2C4O2	143.21	140.68	141.45	139.94	72.58	92.47	68.21
μ (Debey)	2.438	1.589	2.438	1.516	6.382	4.693	7.272

[a] A and B stand for calculations at the B3LYP and MP2 levels, using 6-311++G(d,p) basis set, respectively; R, bond length; ϕ, bond angle; Δ, dihedral angle, and μ, dipole moment.

TABLE 2. ΔG° and Keq for Ket1 Ket2 reaction

	ΔG° (kcal/mol) [14]		K_{eq}	
	A	**B**	**A**	**B**
Gas	-	-	-	-
CCl_4	0.3414	-	0.83	-
CH_3CN	-0.7361	-0.2799	3.46	1.60
H_2O	-0.7549	-0.4606	3.58	2.18

[a] A, and B stand for calculations at the B2PLYP/6-31+G(2d,p), and CBS-QB3, respectively.

TABLE 3. Theoretical and experimental vibrational spectra of keto form of AA (Ket2) along with band assignments. [a]

Theoretical					Experimental				Assignments
F_h	F_a	I_{IR}	R_a	dp	IR[TW][b]	IR[29]	Raman[29]	[29]	PED (%) [TW]
3009	2995	11	113	.58					$vaCH_3$(81), $nsCH_3$(12)
3009	2995	21	154	.74					$vaCH_3$(82), $naCH_2$(19) $nsCH_3$(10)
2966	2950	8	194	.69					$vaCH_3$(64), $nsCH_3$(8), $naCH_2$(19)
2962	2942	6	121	.72					$vaCH_3$(76), $nsCH_3$(10)
2956	2945	1	52	.75					$vaCH_2$(57), $naCH_3$(25)
2916	2925	5	487	.03					$vsCH_2$(63),$nsCH_3$(21)
2907	2921	.2	49	.04					$vsCH_3$(60), $naCH_3$(21), $nsCH_2$(13)
2906	2908	1	388	.01					$vsCH_3$(59), $naCH_3$(21), $nsCH_2$(14)
1729	1725	450	30	.30	1728(100)	1727 vs	1719 m,p	vsC=O	vsC=O(39), $vC\text{-}CH_3$(11)
1707	1702	287	30	.72	1709(69)	1707 vs	1697 w,dp	vaC=O	vaC=O(40), $vC\text{-}CH_3$(10)
1439	1436	21	12	.74	1434(16)	1435 s	1435 m,dp	δaCH_3+CH_2 sci.	δaCH_3(55), $dsCH_3$(12), CH_2 sci (11)
1439	1414	28	7	.67	1434	1435			δaCH_3(60), $dsCH_3$(10) , CH_2 sci (10)
1429	1429	31	21	.71	1434	1435			δaCH_3(52), $dsCH_3$(13), CH_2 Sci(14)
1426	1361	30	17	.54	1422(37)	1435			δaCH_3(61), $dsCH_3$(10)
1412	1396	33	16	.74	1404(24)		1419 m,dp	δaCH_3+CH_2 sci.	CH_2 sci(31), $daCH_3$(21)
1360	1354	75	3	.72	1362(87)	1362 s	1364 w,dp	δsCH_3	δsCH_3(53), $daCH_3$(18)
1358	1349	68	4	.74	1362	1362	1364		δsCH_3(50), $daCH_3$(15), $vC\text{-}CH_3$(14)
1297	1278	172	14	.73	1304(33)	1310 m	1302 m,dp	ωCH_2	ωCH_2(33), naC-C(16), $\delta C{=}O$(14)
1238	1208	36	7	.69	1237(3)	1250 w	1251 m,dp	vaCCC	τCH_2(23), $\delta C{=}O$(14), $vC\text{-}CH_3$(10)
1171	1148	27	9	.52	1171(16)	1171*		ρaCH_3	τCH_2(20), δCO(12), ρCH_3(10)
1151	1139	130	5	.57	1154(17)	1159 m	1166 m,dp	ρaCH_3	ρCH_3(16), δCO(19), ωCH_2(12)
1052	1051	5	4	.34					ρCH_3(23), πCH_3(18), γCO(16)
1034	1032	1	1	.69		1040 w	1043 m,dp	ρsCH_3	πCH_3(27) , γCO(17)
						1020 w		$vaCCH_3$	

946	930	17	7	.23	945(4)	998 vw		ρaCH$_3$	πCH$_3$(19), νC-CH$_3$(14), ωCH$_2$(10) , ρCH$_2$(10)
						970 w	970 w,dp	ρCH$_2$	
941	944	11	4	.36	945	905 vw	900 w,p	vsCCH$_3$	ρCH$_3$(26), πCH$_3$(16), τCH$_2$(16)
832	840	2	4	.75	831vvw				νC-C(14), νC-CH$_3$(16), ρCH$_3$(21), πCH$_3$(16)
806	785	3	7	.34	802(4)				νC-C(10), νC-CH$_3$(12), ρCH$_3$(14), πCH$_3$(15)
782	782	1	16	.03	-	790 w	795 s,p	vsCCC	πCH$_3$(19),nsC-C(12), ρCH$_2$(10)
616	614	5	14	.17	620(2)	623 vvw	627 vs,p	δC-C-C	δC=O(19), γC=O(12), πCH$_3$(10)
							543 w,dp		
528	524	38	5	.72	530(20)	530 w	530 w,dp		δC=O(34), ρCH$_3$(10)
486	484	6	4	.25	484 sh*[b]				γC=O(25),δC=O(15), πCH$_3$(10)
466	472	3	1	.62	472 vw*[b]				γC=O(56)
							412 vw		
377	404	2	1	.52			394 ? w,p		δCCH$_3$(42), δCC(14), ρCH$_2$(10)
							340 w,dp		
318	307	3	1	.33	330w*[b]				δCCH$_3$(54), ρCH$_3$(19)
154	125	4	1	.62					γC=O(20), δCCC(16), δC=O(13), ρCH$_2$(15)
115	231	.1	.1	.71					τCH$_3$(99)
100	NC	.3	.4	.74			75,sh‡		τCH$_3$(99)
62	NC	10	4	.75			60, sh‡		τCH$_3$CO-(99)
36	NC	3	2	.75					τCH$_3$CO-(99)

[a] Fh and Fa, harmonic (scaled) and anharmonic vibrational wavenumbers, respectively, calculated at the B3LYP/6-311++G** level in H_2O solution; I_{IR} and R_a, IR intensity (in km/mol) and Raman activity (in Å^4/amu), respectively; dp, stands for depolarization ratio;v, very; w, weak; S, strong; ν, stretching; δ, in-plane-bending; γ, out-of-plane bending; τ, torsion; ω, wagging; ρ, in-plane rocking; π, out-of-plane rocking; sci, scissoring, τ, twisting; NC, not converged; *, FarIR signals; ‡ TW, this work; [b] In CH_3CN.

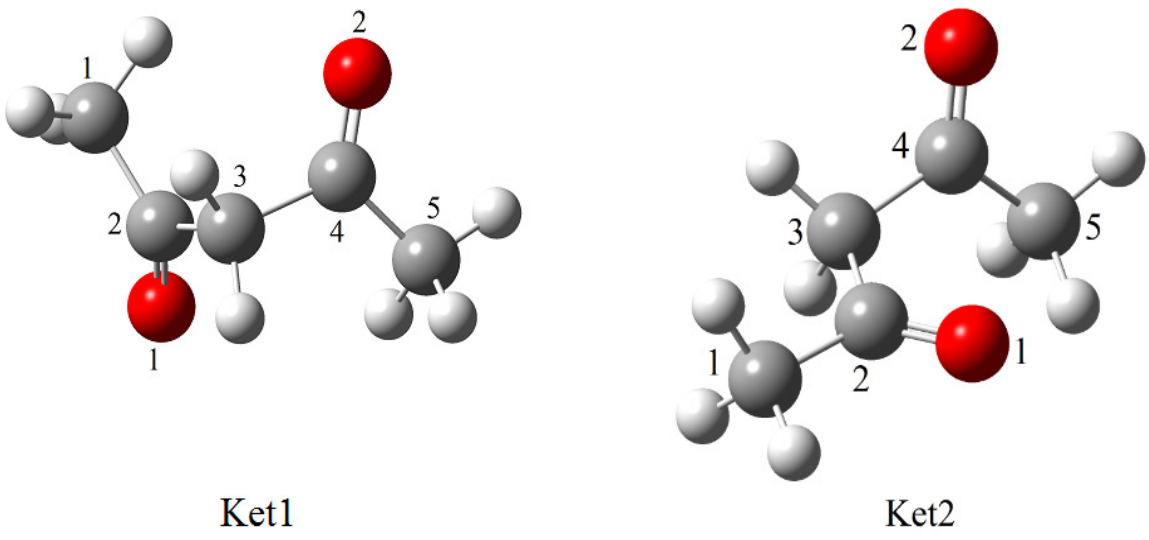

Figure 1. The structure and atom numbering of AA's keto forms.

Figure 2

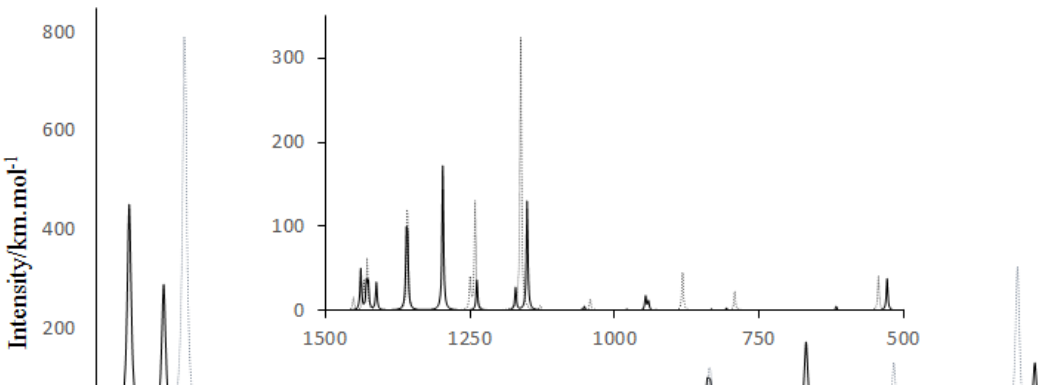

Figure 3

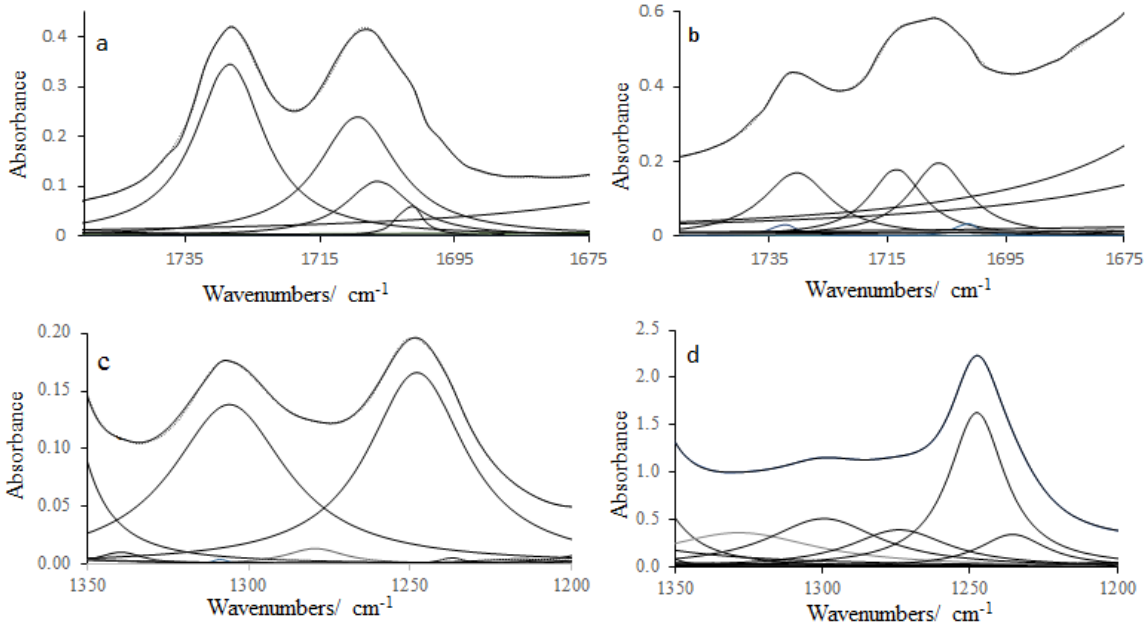

Figure 3. Deconvoluted IR spectra of AA in the CH_3CN (a and c) and CCl_4 (b and d) solutions.

Figure 4

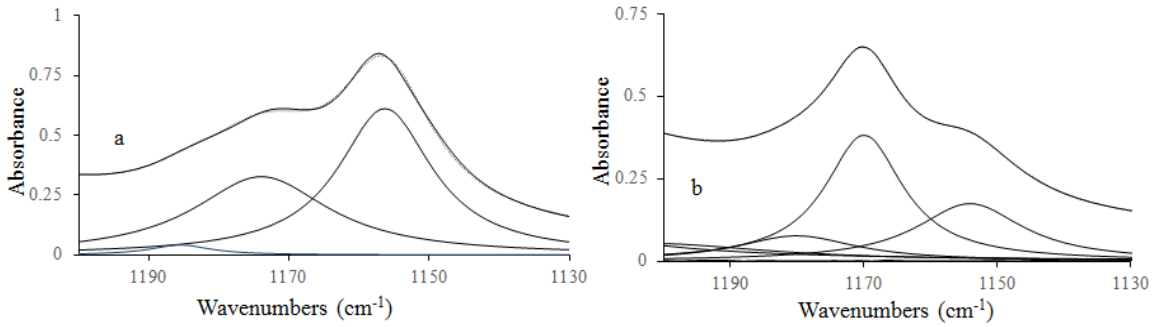

Figure 4. Deconvoluted IR spectra of AA in the CH_3CN (a) and CCl_4 (b) solutions.

to one of the enol bands, δCHα, the 1170 cm^{-1} band is considered as the superposition of one of the Ket1 bands and one of the Ket2 bands, and the 1154 cm^{-1} band is aroused by coupling between C=O bending, CH_2 wagging, and CH_3 rocking modes in Ket2.

Ernstbrunner [29] considered a band at 905 cm^{-1} as one of the keto form vibrational bands. According to our calculations, this band belongs to Ket1 form. In fact, the 944 cm^{-1} band, which is the superposition of two vibrational modes and hidden below the broad OH out-of-plane bending of enol form, belongs to the ket2 species.

The strong Raman band at 795 cm^{-1} [29] is the superposition of ket1 and ket2 bands, such that in both of them the symmetric CCC stretching is highly contributed.

The medium IR band at 530 cm^{-1} is assigned to the in-plane C=O bending and the two weak IR bands at 480 and 472 cm^{-1} are mainly engaged to the out-of-plane C=O bending mode.

Conclusion

In this paper, the relative stabilities of two keto forms of AA are analyzed using the CBS-QB3 and B2PLYp/6-31+G(p,d) and IR spectroscopy. The harmonic and anharmonic vibrational wavenumbers of both keto forms of AA are calculated at the B3LYP/6-311++G** which are in good agreement with the observed band frequencies. We use B3LYP/6-311++G(p,d) level to calculate the internal coordinates of vibrational modes of keto forms of AA. These internal coordinates are utilized for normal coordinate analysis of vibrational band frequencies and potential energy distributions (PED). We described the vibrational frequencies with a high degree of accuracy using PEDs. Also, our calculations show the solvent effect on the Keto forms, in the polar solution Ket2 dipole moment is higher than that for Ket1, which causes the stability of Ket2 in the polar solution to be higher than that of ket1. Comparing the IR spectra of AA in the CCl_4 and CH_3CN solutions reveals coexisting of both keto forms in the sample. However, the relative contents of these two keto forms are solvent dependent, which confirms the theoretical results.

Acknowledgements

The current work is a part of the first author Ph.D thesis which financially supported by Islamic Azad University/Mashhad Branch. We appreciate all professors and students of chemistry department of Islamic Azad University/Mashhad Branch.

References

1. Burdett J. L., Rogers M. T., Keto-Enol Tautomerism in β-dicarbonyls studied by nuclear magnetic resonance Spectroscopy. III. Studies of proton chemical shifts and equilibrium constants at different temperatures. *J. Phys. Chem*, **70**, 939-941 (1966).
2. Mines G. W., Thompson H., Infrared and photoelectron spectra, and keto-enol tautomerism of acetylacetones and acetoacetic esters. *Proc. R. Soc. Lond. A*, **342**, 327-339 (1975).
3. Belova N.V., Oberhammer H., Trang N. H., Girichev G. V., Tautomeric Properties and Gas-Phase Structure of Acetylacetone. *J. Org. Chem*, **79**, 5412–5419 (2014).
4. Park Y. K., Turner C. H., Dose solvent density play a role in the keto-enol tautomerism of acetylacetone?. *J. Supercrit. Fluids*, **37**, 201-208 (2006).
5. Folkendt M. M., Weiss-Lopez B. E., Chauvel J. P., True J. r. N. S., Gas-phase proton NMR studies of keto-enol tautomerism of acetylacetone, methyl acetoacetate, and ethyl acetoacetate. *J. Phys. Chem*, **89**, 3347-3352 (1985).
6. Temprado M., Roux M. V., Umnahanant P., Zhao H., Chickos J.S., The thermochemistry of 2,4-pentanedione revisited: Observance of a nonzero enthalpy of mixing between tautomers and its effects on enthalpies of formation. *J. Phys. Chem, B*. **109**, 12590-12595 (2005).
7. Johnson M. R., Jones N.H., Geis A., Horsewill A.J., Trommsdorff H.P., Structure and dynamics of the keto and enol forms of acetylacetone in the solid state. *J. Chem. Phys*, **116**, 5694-5700 (2002).
8. Cook A.G., Feltman P.M., Determination of solvent effects on keto-enol equilibrium of 1,3-dicarbonyl compounds using NMR. *J. Chem. Educ*, **84**, 1827-1829(2007).
9. Emsley J., Freeman N. J., β-diketone interactions: Part 5. Solvent effects on the keto⇌enol equilibrium. *J. Mol. Struct*, **161**, 193-204 (1987).
10. Sandusky P. O., Expansion of the classic

Acetylacetone physical chemistry laboratory NMR experiment: correlation of the enol-keto equilibrium position with the solvent dipole moment. *J. Chem. Educ*, **91**,739-742 (2014).

11. Powling J., and Bernstein H. J., The Effect of Solvents on Tautomeric Equilibria. *J. Am. Chem. Soc*, **73**, 4353–4356–4356 (1951).

12. Reichardt C., Solvents and Solvent Effects in Organic Chemistry. chap. 4, *Wiley-VCH*, 629 (2004)

13. Emsley J., Freeman N.J., β-diketone interactions: Part 5. Solvent effects on the keto - enol equilibrium. *J. Mol. Struct*, **161**,193-204 (1987).

14. Wetz F., Routaboul C., Lavabre D., Garrigues J.C., Rico-Latters I., Pernet I., Denis A., Photochemical behavior of a new long-chain Uv absorber drived from 4-tert-Butyl-4′- methoxydibenzoylmethane. *Photochem Photobiol*, **80**, 316-321 (2004).

15. Urbaniak W., Jurek K., Witt K., Goraczko A., Staniszewski B., Properties and application of diketones and their derivatives. *Chemik*, **65**, 273-282 (2011).

16. Dračínský M., Čechová L., Hodgkinson P., Procházková E. and Janeba Z., Resonance-assisted stabilisation of hydrogen bonds probed by NMR spectroscopy and path integral molecular dynamics. *Chem. Commun*, **51**, 13986-13989 (2015).

17. Dolati F., Tayyari S. F., Vakili M., Wang Y. A., proton transfer in acetylacetone and its α- halo-derivatives. *Phys. Chem. Chem. Phys*, **18**, 344-350 (2016).

18. Tayyari S.F., Zahedi-Tabrizi M., Azizi-Toopkanloo H., Hepperle S. S., Wang Y. A., The nature of intramolecular hydrogen bond in 2-nitromalonaldehyde. *Chem. Phys*, **368**, 62-65 (2010).

19. Tayyari S. F., Moosavi-Tekyeh Z., Zahedi-Tabrizi M., Eshghi H., Emampour J. S., Rahemi H., Hassanpour M., Intramolecular hydrogen bonding in 2-nitromalonaldehyde: Infrared spectrum and quantum chemical calculations. *J. Mol. Struct*, **782**, 191-199 (2006).

20. Tayyari S. F., Milani-Nejad F., On the reassignment of Vibrational frequencies of Malonaldehyde. *Spectrochim. Acta Part A*, **54**, 255-263 (1998).

21. Tayyari S.F., Milani-Nejad F., Vibrational assignment of Acetylacetone. *Spectrochim. Acta Part A*, **56**, 2679-2691 (2000).

22. Tayyari S.F., Vakili M., Nekoei A.R., Rahemi H., Wang Y. A., Vibrational Assignment of Trifluorobenzoylacetone. A density functional theoretical study. *Spectrochim. Acta Part A*, **66**, 626–636 (2007).

23. Tayyari S.F., Zahedi-Tabrizi M., Afzali R., Laleh S., Mirshahi H.A. and Wang Y. A., Structure and vibrational assignment of the enol form of 3-chloro-pentane-2,4-dione. *J. Mol. Struct*, **873**, 79-88 (2008).

24. Tayyari S.F., Najafi A., Lorestani F., Samelsson R.E., Intramolecular hydrogen bonding in 3-Methylthio-pentane-2,4-dione. *J. Mol. Struct. (Theochem),* **854**, 54-62 (2008).

25. Tayyari S.F., Moosavi-Tekyeh Z., Soltanpour M., Brenji A., Sammelson R.E., Structure and vibrational assignment of 3-nitro-2,4-pentanedione. A density functional theoretical study. *J. Mol. Struct*, **892**, 32-38 (2008).

26. Mauney D., Maner J., McDonald D.C., Duncan M. A., Infrared Spectroscopy of Protonated Acetylacetone and Mixed Acetylacetone/water Clusters. *70th International Symposium on Molecular Spectroscopy*: *at The University of Illinois at Urbana-Champaign*, June 22-26 (2015).

27. Dolati F., Tayyari S.F., Vakili M., Tautomerism, conformational analysis, and spectroscopy studies of 3-bromo-pentane-2,4-dione. *J. Mol. Struct*, **1094**, 264-273 (2015).

28. Dolati F., Tayyari S.F., Vakili M., Wang Y.A., Two-dimensional potential surface for proton transfer in acetylacetone and its α-halo-derivatives. *J. Physical Chemistry Chemical Physics*, **18**, 344-350 (2016)

29. Ernstbrunner E. E., Vibrational Spectra of Acetylacetone and its Anion. *J. Chem. Soc. (A)*, 1558-1561 (1970).

30. Matanović I., Došlić N., Anharmonic vibrational spectra of acetylacetone. *Int. J. Quant. Chem*, **106**(6),1367-1374 (2006).

31. Howard D. L., Kjaergaard H.G., Huang J., Meuwly

M., Infrared and Near-Infrared Spectroscopy of Acetylacetone and Hexafluoroacetylacetone. *J. Phys. Chem*. A, **119** (29), 7980–7990 (2015).

32. Wierzchowski K.L., Shugar D., Infrared spectra of cyanoacetylacetone and the free enolate ions of acetylacetone and cyanoacetylacetone. *Spectrochim. Acta*, **21**(5), 943-954 (1965).

33. Chiavassa T., Verlaque P., Pizzala L., Roubin P., Vibrational studies of methyl derivatives of malonaldehyde: determination of a reliable force field for β-dicarbonyl compounds. *Spectrochim. Acta A*, **50**, 343-351 (1994).

34. Ogoshi H., Nakamoto K., Normal-Coordinate Analyses of Hydrogen-Bonded Compounds. V. The Enol Forms of Acetylacetone and Hexafluoroacetylacetone. *J. Chem. Phys*, **45**, 3113 (1966).

35. Ishida T., Hirata F., Kato K., Thermodynamic analysis of the solvent effect on tautomerization of acetylacetone: An ab initio approach. *J. Chem. Phys,* **110**, 3938-3945 (1999).

36. Cuong N.T., Long K., Van D.U., Effect of solvents on tautomeric equilibrium of acetyl acetone: A Theoretical study. *J. Chem,* **44**, 249-254 (2006).

37. Roy P., Biswas S., Pramanik A., Sarkar P., Computational studies on the keto-enol tautomerism of acetylacetone. *Int. J. Res. Social. Nat. Sci,* **2**, 2455-5916 (2017).

38. Schlund S., Basílio Janke E.M., Weisz K., Engels B., Predicting the tautomeric equilibrium of acetylacetone in solution. I. The right answer for the wrong reason?. *J. Comput. Chem,* **31**, 665-670 (2009).

39. McCann B. W., McFarland S., Acevedo O., Benchmarking continuum solvent models for keto−enol tautomerizations. *J. Phys. Chem. A,* **119**, 8724-8733 (2015).

40. Gaussian 09, Revision A.02, Frisch M. J., Trucks G. W., Schlegel H. B., Scuseria G.E., Robb M. A., Cheeseman J.R., Scalmani G., Barone V., Mennucci B., Petersson G.A., Nakatsuji H., Caricato M., Hratchian X. Li., H. P., Izmaylov A. F., Bloino J., Zheng G., Sonnenberg J.L., Hada M., Ehara M., Toyota K., Fukuda R., Hasegawa J., Ishida M., Nakajima T., Honda Y., Kitao O., Nakai H., Vreven T., Montgomery J. A., Peralta Jr. , J. E., Ogliaro F., Bearpark M., Heyd J. J., Brothers E., Kudin K. N., Staroverov V. N., Kobayashi R., Normand J., Raghavachari K., Rendell A., Burant J. C., Iyengar S.S., Tomasi J., Cossi M., Rega N., Millam J. M., Klene M., Knox J. E., Cross J. B., Bakken V., Adamo C., Jaramillo J., Gomperts R., Stratmann R. E., Yazyev O., Austin A.J., Cammi R., Pomelli C., Ochterski J.W., Martin R.L., Morokuma K., Zakrzewski V.G., Voth G. A., Salvador P., Dannenberg J. J., Dapprich S., Daniels A.D., Farkas Ö., Foresman J.B., Ortiz J.V., Cioslowski J. and Fox D. J., Gaussian, Inc., Wallingford CT, (2009).

41. Becke A., Density-functional thermochemistry. III. The role of exact exchange. *J. Chem. Phys*, **98**,5648 (1993).

42. Lee C., Yang W. and Parr R.G., Development of the Colle-Salvetti correlation-energy formula into a functional of the electron density. *Phys. Rev*, *B*, **37**, 785-89 (1988).

43. Stephens P. J., Devlin F. J., Chabalowski C. F., Frisch M. J., Ab Initio Calculation of Vibrational Absorption and Circular Dichroism Spectra Using Density Functional Force Fields. *J. Phys. Chem,* **98**, 11623-11627 (1994).

44. Cossi M., Scalmani G., Rega N. and Barone V., New developments in the polarizable continuum model for quantum mechanical and classical calculations on molecules in solution. *J. Chem. Phys*, **117**, 43-54 (2002).

45. Tomasi J., Mennucci B. and Cammi R., Quantum mechanical continuum solvation models. *Chem. Rev*, **105**, 2999-3093 (2005).

46. Wood G. P. F., Radom L., Petersson G. A., Barnes E.C., Frisch M. J., and Montgomery J. A., Jr., A restricted-open-shell complete-basis-set model chemistry. *J. Chem. Phys*, **125**, 094106 (2006).

47. Grimme S., Semiempirical hybrid density functional with perturbative second-order correlation. *J. Chem. Phys*, **124**,034108 (2006).

48. Denis P.A., Coupled cluster, B2PLYP and M06-2X investigation of the thermochemistry of five-membered nitrogen containing heterocycles, furan, and thiophene. *Theor. Chem. Acc,* **129**,

219–227 (2011).

49. El-Nahas A. M., Simmie J. M., Navarro M. V., Bozzelli J. W., Black G., Curran H. J., Thermochemistry and kinetics of acetonylperoxy radical isomerisation and decomposition: a quantum chemistry and CVT/SCT approach. *Phys. Chem. Chem. Phys,* **10**, 7139-7149 (2008).

50. Pickard IV F. C., Pokon E.K., Liptak M.D., Shields G.C., Comparison of CBS-QB3, CBS-APNO, G2, and G3 thermochemical predictions with experiment for formation of ionic clusters of hydronium and hydroxide ions complexed with water. *J. Chem. Phys*, **122**,024302 (2005).

51. Barone V., Anharmonic vibrational properties by a fully automated second-order perturbative approach. *J. Chem. Phys*, **122**,014108 (2005).

52. Tayyari S.F., Bakhshi T., Mahdizadeh S.J., Mehrani S., Sammelson E. R., Structure and vibrational assignment of magnesium acetylacetonate: A density functional theoretical study. *J. Mol. Struct*, **938**, 76-81 (2009).

53. Omidvar B. A., Tayyari S. F., Vakili M., Nekoei A., Normal coordinate analysis of pyridine and its C_{2v} ^{2}H-isotopomers. A New approach. *J. Mol. Struct*, **1151**, 236–244 (2018).

54. Tayyari S.F., Gholamhoseinpour M., Emamian S., Conformational analysis, structure, and normal coordinate analysis of vibrational spectra of hexafluoroacetone. A density functional theory study. *Fluor. Chem*, **184**, 65-71(2016).

55. Gholamhoseinpour M., Tayyari S.F., Emamian S., Conformational stability, barriers to internal rotations, and normal coordinate analysis of acetone and its ^{2}H-isotopomers. *Can. J. Chem*, **94**, 818-826 (2016).

56. Gunasekaran S., Kumaresan S., Arun Balaji R., Anand G. and Seshadri S., Vibrational spectra and normal coordinate analysis on structure of chlorambucil and thioguanine, *Pramana – J. Phys*, **71**(6), 1291-1300 (2008).

57. Tanveer H., Singh P.K., Singhal K., Raj P. and Neeraj Misra, Normal coordinate analysis and quantum chemical study of tris (*p*-fluorophenyl) antimony di(*N*-phenylglycinate) [(*p*-FC6H4)3Sb(O2CCH2NHC6H5)2]. *Pramana – J. Phys*, **69**(4), 675-680 (2007).

58. GaussView 4. 1. 2, Gaussian Inc., Pittsburg, PA, (2006).